Validation of the Geostationary Lightning Mapper with a Lightning Mapping Array in Argentina: Implications for Current and Future Spaceborne Lightning Observations

Timothy J. Lang[1]
[1]NASA Marshall Space Flight Center, Huntsville, Alabama.

Corresponding author: Timothy Lang (timothy.j.lang@nasa.gov)

Key Points:

- The Geostationary Lightning Mapper detected lightning with overall 75% efficiency relative to a ground network in Argentina.
- Detection efficiency depended significantly on day/night, and on flash rate, size, altitude, and the presence of anomalous lightning.
- An improved sensor that could better detect and distinguish between small flashes would provide more information about storm evolution.

Abstract

A validation study of the Geostationary Lightning Mapper (GLM) on board the Geostationary Operational Environmental Satellite 16 (GOES-16) was done using a ground-based lightning mapping array (LMA) deployed as part of the Remote sensing of Electrification, Lightning, And Mesoscale/microscale Processes with Adaptive Ground Observations (RELAMPAGO) field campaign in Argentina. GLM detected lightning with 74.6% efficiency over 61 thunderstorm days in December 2018 through April 2019. However, GLM detection efficiency (DE) was negatively correlated (r = -0.49) with LMA flash rate. GLM DE also was negatively correlated with LMA flash altitude (r = -0.24), reflecting the influence of multiple competing trends. GLM DE was positively correlated (r = 0.27) with number of LMA sources in a flash, indicating improved DE for larger flashes. During periods with anomalously electrified storms, GLM DE was reduced to 50.9%. Statistics were found to be sensitive to analysis criteria, but most of the above trends remained consistent regardless of specific criteria. Because the methodology allowed a GLM flash to match more than one LMA flash, actual GLM flash rate was a factor of 2.9 lower than the LMA flash rate, and this ratio grew larger as LMA flash rate increased. A sensitivity study examined the impact of improved DE for smaller flashes; that is, an improved sensor (or algorithm) that was better able to detect and distinguish between separate small lightning flashes. The results showed improved correlation with LMA flash rates, as well as improved ability to identify lightning jumps associated with intensifying convection.

Plain Language Summary

Based on a comparison with a ground-based, three-dimensional lightning detection system in Argentina, the Geostationary Lightning Mapper (GLM) on board the Geostationary Operational Environmental Satellite 16 (GOES-16) detects lightning with nearly 75% efficiency, which meets its requirements. However, that detection efficiency decreases a lot when thunderstorms produce a lot of lightning at once, or small lightning flashes, or when lightning occurs deeper in the cloud where it is more difficult for the optical pulse to make its way to cloud top. This makes GLM somewhat less useful during the most intense part of a storm's life. However, if GLM or a similar sensor could be made more sensitive, either with improved hardware design or better data processing, then it would become more useful in intense storms.

1 Introduction

Ever since the Geostationary Lightning Mapper (GLM) on board the Geostationary Operational Environmental Satellite 16 (GOES-16) first began operating in 2017, it has been recognized as a highly successful instrument that makes critical and continuous observations of lightning across its quasi-hemispheric field of view (Rudlosky et al. 2019). Since then, two additional GLMs – on GOES-17 and -18 – have launched (e.g., Bateman et al. 2021, Rudlosky & Virts 2021). Due to its continuous monitoring capability, GLM regularly observes far more lightning than its predecessors. For example, the Lightning Imaging Sensor (LIS), which has been hosted on the Tropical Rainfall Measuring Mission (TRMM; Kummerow et al. 1998) and the International Space Station (ISS; Blakeslee et al. 2020), provided much of the design heritage for GLM (in particular, the focus on the 777.4-nm oxygen triplet, which enables optical detection of lightning during daytime; Goodman et al. 2013), but due to its low-Earth orbit (LEO) cannot

observe in raw numbers as much lightning as GLM. LIS, along with its predecessor the Optical Transient Detector (OTD; Christian et al. 2003), has been aimed at documenting global lightning, which GLM cannot do.

However, because it views continuously and observes so much lightning, issues have been noted with GLM that were not as well-documented with previous spaceborne lightning mappers, despite the common design heritage. One major area of concern has been false alarms; that is, event detections that do not correspond to actual lightning (Bateman & Mach 2020, Peterson 2020, Bateman et al. 2021). These often manifest as solar glint (either off clouds or reflective surfaces like water), or artifacts manifested by GLM electronics (e.g., "Bahama bars"; Bateman & Mach 2020). However, though they are challenging to address in processing algorithms, it is relatively straightforward to document these issues, as reference ground- and space-based datasets exist for cross-check (though challenges still remain; Virts & Koshak 2023). Moreover, false alarms often are dependent on relatively predictable patterns (e.g., solar reflections as the sun moves across the GLM field of view). Also, false alarms don't seem to be as large of a concern in LEO missions like LIS (Blakeslee et al. 2020, Lang & Bang 2022).

Perhaps more concerning, then, is the lightning that GLM (and by extension, other missions that use the 777.4 nm detection capability) may miss. GLM was designed to provide 70% minimum detection efficiency (DE) averaged across the field of view (Goodman et al. 2013). This is likely as good or better than what TRMM LIS was able to provide, and is better than the ~60% DE provided by ISS LIS (Blakeslee et al. 2020). But not all lightning is created equal, and GLM (and related missions') DE may be a strong function of lightning type and thunderstorm evolutionary state (Murphy & Said 2020, Rutledge et al. 2020, Zhang & Cummins 2020, Peterson 2021a).

One of the critical services that GLM provides is continuous monitoring of severe storms. A notable feature of severe storms is their propensity to produce a lot of lightning flashes, particularly while intensifying prior to the production of strong winds, hail, or tornadoes. This so-called "lightning jump" (Williams et al. 1999, Schultz et al. 2009, Gatlin & Goodman 2010, Chronis et al. 2015) was originally identified using three-dimensional total lightning mappers that detect close to 100% of the lightning within their range (~100 km). The lightning jump is clearly linked to significant kinematic and microphysical changes in thunderstorms as they evolve (Chronis et al. 2015, Schultz et al. 2015, 2017). One change that is very common is increased updraft strength, which leads to increased frequency of small-scale turbulent eddies that separate charge over smaller distances, subsequently encouraging smaller flashes near updrafts compared to further away (Bruning & MacGorman 2013, Schultz et al. 2015).

To summarize, then, intense or severe thunderstorms are highly likely to produce a lot of small lightning flashes near their updraft cores. However, these flashes are also the kind of lightning that GLM is most likely to miss. This is because the flashes may produce a reduced amount of optical energy, and they may fall below the horizontal spatial resolution of GLM (~8-10 km). And due to the design heritage, there is no reason to think that similar instruments like LIS would not be similarly challenged (Zhang & Cummins 2020).

An additional issue is anomalous storms; that is, storms that tend to have a preponderance of positive electrical charge at mid-levels (roughly -10 to -20 °C) compared to typical storms (Rust et al. 2005; Wiens et al. 2005; Bruning et al. 2014). A major consequence of this is most of the lightning in these storms occurs lower in altitude within the cloud. This naturally limits the amount of optical scattering reaching cloud top, upon which imagers like GLM, LIS, etc. depend (Marchand et al. 2019, Rutledge et al. 2020, Peterson et al. 2021).

Thus, the focus of this study will be on quantitatively documenting how GLM-16 DE evolves as lightning and thunderstorms evolve. This will enable us to understand how to properly interpret GLM (and similar) observations when DE is expected to be challenged (e.g., small flashes in severe storms, anomalous storms, etc.). The domain of interest is a three-dimensional (3D) lightning mapping network in north-central Argentina, which was deployed in support of the Remote sensing of Electrification, Lightning, And Mesoscale/microscale Processes with Adaptive Ground Observations (RELAMPAGO) field campaign (Nesbitt et al. 2021). GLM performance in this domain was studied by Lang et al. (2020); however, that study only examined two cases. The present study will build on this to examine a multi-month period, enabling a high level of statistical confidence in the results. Argentina is an excellent domain to study because severe weather is relatively common there (Nesbitt et al. 2021), and anomalous storms also can occur (Medina et al. 2022).

While this study will focus on GLM-16, its results will be relevant to similar missions. This includes current geostationary instruments like GLM-17/18, Lightning Mapping Imager (LMI; Cao et al. 2021), and Meteosat Third Generation Lightning Imager (MTG-LI; Holmlund et al. 2021). It also includes LEO missions like LIS (both TRMM and ISS), OTD, Fast On-orbit Recording of Transient Events (FORTE; Suszcynsky et al. 2001), and the Atmosphere-Space Interactions Monitor (ASIM; Neubert et al. 2019). Ultimately, any instrument focused on measuring lightning via the 777.4-nm optical emission band is going to be affected by day/night asymmetries in DE, as well as challenges in detecting small, optically dim flashes, or lightning occurring within optically thick clouds.

It should be noted that ASIM also monitors lightning at 337 nm (Chanrion et al. 2019). This ultraviolet (UV) band is typically more sensitive to colder streamer activity, compared to 777.4 nm which is more sensitive to hotter leader activity. Indeed, there appears to be a population of lightning flashes that are predominantly more detectable at 337 vs. 777 nm (Soler et al. 2021). Similarly, there are flashes that are more readily detectable in radio frequency (RF) compared to optical frequencies (e.g., Jacobson & Light 2012). These flash detectability differences have important implications for single-channel sensors like GLM, LIS, etc. Specifically, a multi-frequency approach may yield important detectability improvements that allow overall a more representative population of lightning flashes to be detected. This could have benefits for algorithms based on phenomena like lightning jumps. Thus, it would be helpful to understand what benefits may accrue based on improved DE of additional lightning flashes.

2 Data and Methods

2.1 Geostationary Lightning Mapper (GLM)

For this study, the GLM on GOES-16 was used. This sensor has already undergone a validation process (e.g., Bateman & Mach 2020, Quick et al. 2020, Virts & Koshak 2020) by the National Aeronautics and Space Administration (NASA) and the National Oceanic and Atmospheric Administration (NOAA); however, it remains useful to continue probing potential limitations of the instrument, so that its full scientific potential can be understood. This study used the Level 2 datasets provided by the Lightning Cluster Flash Algorithm (LCFA; GOES-R 2018), which identifies Flashes as a collection of Groups, and Groups as a collection of Events (Mach 2020). There is significant evidence that the LCFA erroneously breaks up very large, long-duration stratiform lightning flashes (“megaflashes”; Peterson 2019, 2021b), mainly due to

159 computational optimizations that improve realtime latency. This issue leads to the identification
160 of multiple flashes when in reality there was only a single megaflash. However, because such
161 flashes are rare (< 1% of the GLM dataset), they should not influence the results of this study.
162
163 2.2 Lightning Mapping Array (LMA)
164
165 The RELAMPAGO LMA was deployed during November 2018 through April 2019; i.e.,
166 the austral warm season. The centroid of the LMA was near the city of Córdoba, Argentina.
167 LMAs map lightning in 3D using Global Positioning System (GPS) time-of-arrival techniques
168 (Rison et al. 1999), and are generally considered to detect nearly all lightning within relatively
169 close range of network center (e.g., Thomas et al. 2004). The network consisted of up to 11
170 stations during this time; however, the number of stations operating on a given day was variable.
171 Generally at least 7 stations were operational, and more typically 9+. The published
172 RELAMPAGO LMA Level-2 dataset was used in this study (Lang 2020). This dataset consists
173 of individual VHF source locations as well as identified flashes using the processing approach by
174 Lang et al. (2020). The main constraints on the flash identification were a maximum of 150 ms
175 and 3 km between successive sources in a flash, and a flash could have a 3-s maximum duration.
176 LMA flashes were defined using thee different minimum thresholds – 3, 10, and 100 points – in
177 order to explore the impact of smaller vs. larger flashes on GLM DE. Because the LMA was still
178 being installed and improved during significant portions of November, this study focused on the
179 December-April period.
180
181 2.3 Analysis Methodology
182
183 This study focused only on lightning within 100 km of the RELAMPAGO LMA
184 centroid, as Lang et al. (2020) found that LMA performance was optimized within this region.
185 This occurred on 61 thunderstorm case days during December-April deployment (i.e., one or
186 more thunderstorms occurred roughly every other day). There were additional days with only 1-2
187 LMA flashes (1 January, 2 and 25 February) that were excluded from this total. Though 26
188 December had LMA lightning, GLM observations were missing for the relevant time period, so
189 this day also was excluded from analysis.
190 For the statistical validation, the main time unit for determining flash rates was 10
191 minutes. Besides being conveniently equal to the 10-minute data files provided by the LMA
192 processing algorithm (Lang 2020), this also reduced noise and focused on broad-based flash and
193 instrument performance trends within the 100-km radius domain. A GLM flash matched an
194 LMA flash if its centroid occurred within 500 ms and 25 km of at least one LMA flash. Due to
195 the fundamentally different nature of the GLM (optical) and LMA (VHF) measurements, as well
196 as the coarser ~10-km resolution of GLM, a GLM flash was allowed to match multiple LMA
197 flashes if the time and distance criteria above were all met. This benefitted GLM DE even if
198 GLM flash rates in the domain were well below LMA flash rates. Sensitivity studies were
199 performed with these spatiotemporal matching criteria halved (250 ms and 12.5 km) and doubled
200 (1000 ms and 50 km). GLM flashes were initially restricted to 150 km of LMA centroid before
201 performing any spatiotemporal matching. This allowed GLM flashes just outside the 100-km
202 radius of analysis to match with LMA flashes inside the radius.
203 Day (1100-2200 UTC) and Night (0000-0830 UTC) were broken out, with transition
204 periods (2200-0000 and 0830-1100 UTC) only included in Overall statistics. The transition

periods were made wide enough to exclude any seasonal changes in sunrise/sunset during December-April. For example, around austral summer solstice daytime is longer than 1100-2200 UTC, but this is not true after the austral autumnal equinox.

Sensitivity studies were done that examined the possible benefits of improved GLM (or GLM-like) DE of missed flashes. This simulated the impacts of 0-100% improvement in the identification of missed LMA flashes by a spaceborne sensor; that is, an improved sensor or algorithm that was able to resolve (and thus match) additional individual small LMA flashes. This could include flashes that were fully missed by GLM, as well as more than one of the multiple LMA flashes that were allowed to match a single GLM flash. In the latter case, this simulated an improved ability by a spaceborne instrument to resolve these individual small, weak flashes that are captured by the LMA without amalgamating them into a single, lower-resolution optical flash seen by GLM. For the above analysis, 1-minute flash rates within 100-km of the LMA were calculated for both GLM and the LMA on all case days analyzed for the statistical DE study (which was done at 10-minute resolution, see above).

Lightning jumps (LJs) were defined following the methodology of Chronis et al. (2015). Similar to that study, the average 2-minute flash rate of the most recent 14 minutes of lightning was computed, and then the standard deviation of 2-minute flash rates were computed for the most recent 12 minutes. The most recent 2-minute flash rate was then compared to the average, and if it was greater than 3 times the standard deviation above the average, and the flash rate was greater than 25 min^{-1}, then an LJ was identified. Chronis et al. (2015) explored a variety of α (multiplicand of the standard deviation, σ) and absolute flash rate thresholds, and found that LJs correspond to significant kinematic and microphysical changes in a thunderstorm. Analysis by Schultz et al. (2015, 2017) also supported this inference. The present study used α of 3 and the 25 min^{-1} threshold to limit the focus to the strongest LJs, those that were most likely to truly correspond to significant thunderstorm evolution, as opposed to potential noise. After an LJ was identified, 10 minutes were required to pass before another LJ could be identified.

LJs for both the LMA and GLM were computed, with GLM LJs recomputed according to 0-100% improvements in DE as described above. A limitation of this analysis, compared to Chronis et al. (2015) and Schultz et al. (2015, 2017), was that individual thunderstorms were not isolated and tracked. All storms within 100 km were allowed to contribute to the LJ analysis. This is another reason this study only focused on stronger LJs, to limit the effect of a mixture of evolutionary states within multicellular storms on the statistics. In addition, this study did not consider a storm's propensity to produce severe weather relative to an LJ; the focus was solely on significant thunderstorm evolutionary changes within the analysis domain, as indicated by the presence of an LJ.

False alarm rates were not explored in this study, as that would have required also analyzing non-thunderstorm time periods. As discussed earlier, false alarms are a known issue with GLM, but this study was primarily focused on DE as a function of flash rate and flash/thunderstorm behavior. In addition, significant progress has been made on reducing false alarms and artifacts in GLM-16 since 2018-2019 (e.g., Bateman et al. 2021), while reduced DE

during thunderstorm intensification or anomalous periods remains an issue where limited progress has been made (e.g., Rutledge et al. 2020).

3 Results

3.1 Overview

Figure 1 shows an example set of time series exemplifying GLM performance during RELAMPAGO, which helps to motivate this study. Similar figures for other cases can be found in Lang et al. (2020). The case in question here is 23 February 2019, where an intense thunderstorm transited through the southern portion of the LMA domain. Initially, GLM DE was nearly 100% as LMA flash rate was low and flashes tended to have a large (~100 or more) number of points. However, as the storm intensified flashes grew smaller (i.e., fewer points per flash), and LMA flash rates reached a peak of ~80 min^{-1} (averaged over a 10-minute period) at two separate times (during the 0400 and 0500 UTC hours, respectively). Flash rates then weakened (to ~40 min^{-1}) before the storm exited the analysis domain. While GLM was broadly correlated with the LMA, in that it also showed an enhancement and then a reduction in lightning, GLM peak flash rates were more than a factor of 4 lower. This was primarily due to a very large reduction in GLM DE when the thunderstorm intensified, down to less than 20% during part of 0500-0600 UTC. This hour-long time period also corresponded to when the storm appeared to be anomalously electrified, according to Medina et al. (2021); mean source altitude also decreased during this time period. Moreover, due to some complexities in the GLM DE curves, where 100+ point flash DE remained high into the 0400 UTC hour before finally collapsing like the 10+ point DE did an hour earlier, GLM appeared to identify an earlier time period than the LMA as the flash rate maximum (roughly 30 minutes earlier, in fact). In addition, GLM did not resolve the second LMA peak during 0520-0530 UTC.

These single-case results illustrate the major themes of this study. For example, GLM can have high DE (particularly for larger flashes), but when storms are intensifying DE appears to be anticorrelated with actual flash rate. GLM DE also appears to be negatively impacted by transient anomalous periods in thunderstorms. Ultimately, this makes GLM's response in intense and/or anomalous storms much more muted than it ideally should be, limiting the utility of GLM flash rate to identify intense storms (e.g., Murphy & Said 2020).

The remainder of this Results section will build on this case study, as well as the work of Lang et al. (2020), to explore these themes in much more quantitative and statistical detail. In

addition, the effects of potential improvements in spaceborne optical lightning DE will be explored.

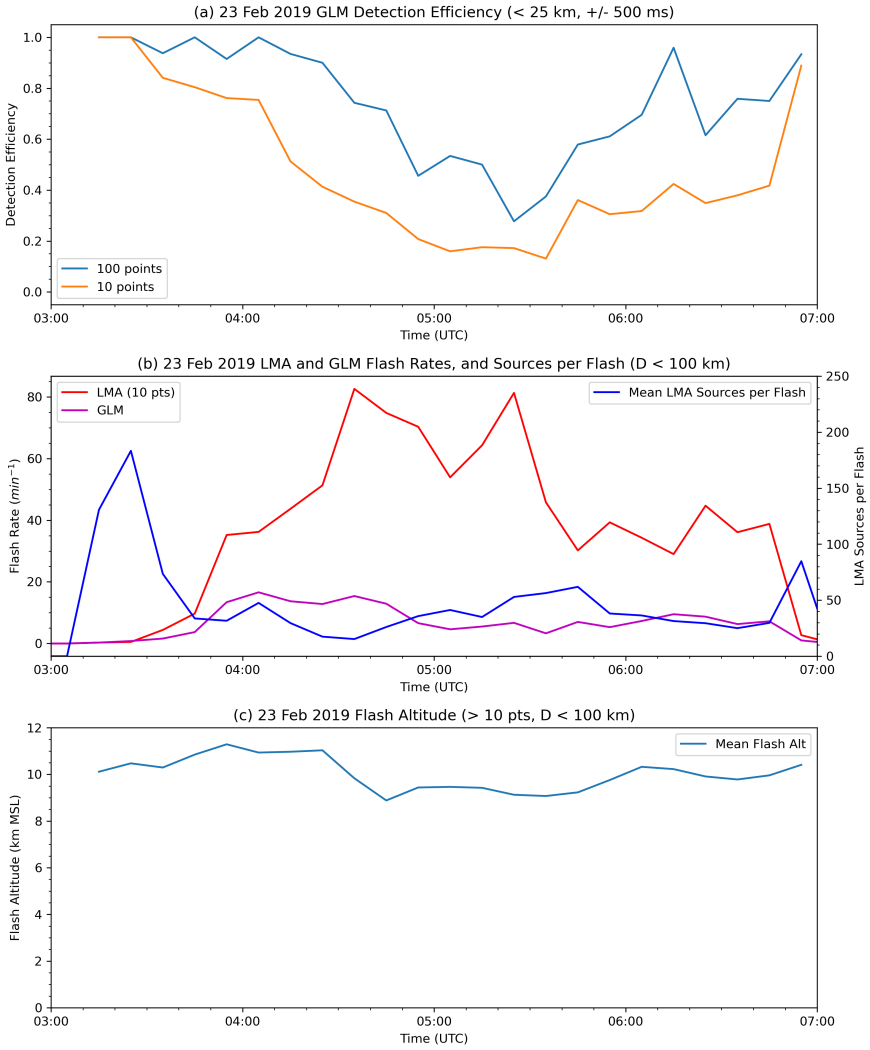

Figure 1. GLM and LMA observations within 100 km of the LMA on 23 February 2019. (a) Time series of GLM DE for LMA-identified flashes with 10+ and 100+ points. (b) LMA and GLM flash rates, and mean LMA sources per flash. (c) Mean LMA flash altitude.

3.2 Statistical Analysis of GLM Detection Efficiency

Between all 61 case days, there were 8762 possible ten-minute periods to enable DE and correlation analyses. Depending on which flash rate was computed (e.g., GLM vs. LMA, 3-point vs. 100-point), the actual number of ten-minute periods with lightning ranged within 2105-2502. Correlations were done assuming these periods with lightning were linked as a continuous time series. This is justified as flash rates nearly always tapered toward 0 near the start and end of

individual cases with lightning. Spearman correlations were computed as these do not assume a linear relationship between the variables, only a monotonic one.

Statistics from the analysis are presented in Table 1. Results are broken out by the standard 25-km and 500-ms matching criteria as well as whether those criteria were halved or doubled. Day, Night, and Overall statistics are also provided. Discussion of this Table will focus on the broader trends. Overall, for a 10-point minimum threshold to define an LMA flash, GLM detected ~75% of LMA lightning, which met GLM's performance requirements (Goodman et al. 2013). Decreasing the threshold to 3-points only hurt DE by 1-5%. Increasing the threshold to 100 points improved DE by ~10-20%. Halving the matching criteria reduced DE by ~10-20% (which reduced GLM well below 70% DE except for 100+ point flashes), while doubling the criteria improved DE by ~5-10%. As expected, GLM performance during daytime was significantly less than nighttime, again ~10-20% worse. GLM DE at night could exceed 90%, depending on matching criteria and LMA points threshold. Overall, the statistics indicated very good overall DE performance by GLM, but this performance was sensitive to specific thresholds used in the analysis.

Medina et al. (2021) identified 38 hourlong blocks (their unit of analysis) during December 2018 through April 2019 when the LMA indicated anomalous lightning behavior. This behavior was determined by the use of an automated charge identification algorithm, called Chargepol, which estimated the polarity, altitude, and vertical depth of charge layers based on bulk flash behavior. Within these 38 hourlong blocks, there were 209 total ten-minute periods with LMA lightning (this was roughly 8-10% of all lightning-producing periods during December-April). Overall DE statistics for these anomalous periods are presented in Table 1. The DE statistics were not further broken down into Day vs. Night due to the reduced sample size. Under the standard matching criteria, for 10+ point LMA flashes DE was reduced to ~51%. This DE was again sensitive to matching criteria and LMA points threshold, but overall ~20-25% decreases in DE were common during anomalous scenarios.

Moving to the Spearman correlations, under the standard criteria (25-km, 500-ms, 10+ points) GLM and LMA flash rates were highly correlated (r = 0.95), and this was largely insensitive to Day vs. Night, as well as halving or doubling of the spatiotemporal matching criteria (0.95-0.97 range). Somewhat counterintuitively (since it improved GLM DE), increasing the LMA points threshold to 100 actually reduced the flash rate correlation, to a range of 0.85-0.89. However, increasing the point threshold that high actually reduced the overall population of LMA flashes by ~70%. In that scenario, the assumptions underpinning the correlation analysis (that flash rates tapered toward zero only near the beginning and end of a given lightning case) became less well-supported. As many studies have noted, flashes tend to become smaller as a thunderstorm intensifies. Thus, the relative fraction of 100+ point flashes should decrease when that occurs, which should act to decorrelate the LMA and GLM time series. This decorrelation trend when using the 100-point threshold can be seen elsewhere in Table 1 as well.

Despite the robustly high correlation between GLM and LMA flash rates, GLM DE was actually significantly anticorrelated with LMA flash rate. The baseline correlation under the aforementioned standard criteria was -0.49, and this was largely insensitive to halving or doubling the spatiotemporal matching criteria, as well as the LMA points threshold (the range was -0.41 to -0.50). What appeared to impact the degree of anticorrelation was Day vs. Night,

with nighttime anticorrelations larger than daytime. The already-reduced GLM DE during daytime appeared to be playing a role in this difference.

Table 1. GLM detection efficiencies and Spearman correlation coefficients vs. the RELAMPAGO LMA under various scenarios. *Correlation not significant at 99% confidence level.

	25 km and 500 ms			12.5 km and 250 ms			50 km and 1 s		
	Day	**Night**	**Overall**	**Day**	**Night**	**Overall**	**Day**	**Night**	**Overall**
GLM DE		*%*			*%*			*%*	
3+ pts/flash	67.2	82.4	73.5	51.0	60.6	54.6	75.7	91.9	82.9
10+ pts/flash	68.1	83.6	74.6	54.3	64.6	58.2	75.9	92.3	83.2
100+ pts/flash	81.2	91.6	85.2	69.2	76.2	71.4	86.1	96.9	90.5
Anomalous GLM DE									
3+ pts/flash			50.6			33.9			63.2
10+ pts/flash			50.9			35.9			63.1
100+ pts/flash			69.1			54.8			77.2
GLM rate vs. LMA rate	*Spearman Correlation*			*Spearman Correlation*			*Spearman Correlation*		
3+ pts/flash	0.95	0.97	0.95	0.95	0.97	0.96	0.95	0.97	0.96
10+ pts/flash	0.95	0.97	0.95	0.95	0.97	0.95	0.95	0.97	0.95
100+ pts/flash	0.85	0.89	0.85	0.85	0.89	0.85	0.85	0.89	0.85
GLM DE vs. LMA rate									
3+ pts/flash	-0.37	-0.61	-0.50	-0.43	-0.49	-0.47	-0.28	-0.52	-0.41
10+ pts/flash	-0.37	-0.60	-0.49	-0.41	-0.46	-0.45	-0.28	-0.53	-0.42
100+ pts/flash	-0.43	-0.58	-0.49	-0.42	-0.42	-0.41	-0.39	-0.57	-0.47
GLM DE vs. LMA altitude									
3+ pts/flash	-0.35	-0.34	-0.34	-0.27	-0.23	-0.25	-0.30	-0.27	-0.29
10+ pts/flash	-0.23	-0.30	-0.24	-0.20	-0.20	-0.18	-0.18	-0.23	-0.19
100+ pts/flash	-0.04*	-0.10	-0.06	-0.06*	-0.10	-0.08	0.02*	-0.06*	-0.01*
GLM DE vs. LMA pts/flash	0.40	0.18	0.27	0.46	0.30	0.37	0.30	0.05*	0.15

GLM DE vs. mean LMA flash altitude was anticorrelated (standard result was -0.24), which is somewhat counterintuitive since previously a reduction of DE during anomalous periods was noted. This was likely due to competing trends, which ultimately summed to a weakly negative overall correlation. Certainly, anomalous periods tend to be associated with lower flash altitudes. However, as Lang et al. (2020) and others have noted, flash altitude can increase during thunderstorm intensification, and as Table 1 shows GLM DE was anticorrelated with LMA flash rate. Finally, larger flashes tended to be more readily detected by GLM, and these flashes are often associated with more stratiform lightning, which often is lower in altitude than lightning contained within deep convection. The influence of these competing trends may also be seen in the increased sensitivity to various matching criteria and points thresholds, where the anticorrelation can range from statistical insignificance to as high as -0.35.

The last row in Table 1 concerns GLM DE vs. mean points per LMA flash. Here, data for 3+ point flashes (i.e., the largest LMA flash dataset used in this study) were examined. The standard correlation was 0.27, and this was highly sensitive (range of 0.05-0.46) to the choice of criteria. In general, criteria that tended to reduce baseline GLM DE (e.g., focusing on Day,

halving spatiotemporal criteria, etc.) usually improved this correlation, while criteria that tended to increase DE (e.g., Night, doubling) reduced the correlation, sometimes to the point of statistical insignificance. Thus, the occurrence of larger flashes (i.e., those with more LMA points) tended to improve DE at the margins, when GLM DE was already being throttled by other restrictions. For example, since nighttime GLM DE during RELAMPAGO was already high to begin with, making flashes a little bit bigger didn't have as strong an effect as during the daytime. This trend is also visible in Table 1's GLM DE entries, where (for example) DE improvements from 10- to 100-point thresholds were greater during Day than Night.

3.3 Investigation of the Impact of Improved GLM Detection Efficiency

As has been demonstrated, GLM DE was significantly anticorrelated with LMA flash rate during RELAMPAGO (Table 1). In addition, the ratio of LMA flashes to GLM flashes seemed to grow larger as flash rate increased (e.g., Fig. 1). Recall that because the flash matching process allowed a single GLM flash to correspond to more than one LMA flash, the absolute ratio of LMA flashes to GLM flashes could be large even if GLM DE was high. For the entire December-April time period, the ratio of LMA flashes to GLM flashes was 2.9:1 (10+ points/flash). The behavior of this ratio as a function of 10-minute-average LMA flash rates is shown in Fig. 2. As can be seen, the ratio increased approximately monotonically with LMA flash rate (Fig. 2a), up to a 10-minute rate of 250 min^{-1}, though the relationship grew noisier as sample size declined at higher flash rates (Fig. 2b). This reflected the mutually reinforcing effects of reduced GLM DE at high flash rates, as well as an increased probability that a single GLM flash would match with more than one LMA flash when LMA rates were high.

The net effect is that GLM response becomes increasingly dampened as LMA flash rates increase to very high values. GLM rate of increase is throttled as storms intensify, as are the absolute flash rates (Fig. 1; Lang et al. 2020). This would be expected to decorrelate GLM and LMA during peak storm intensities, and also could affect the identification of LJs within GLM data.

As discussed in the Introduction, this issue should also affect other spaceborne optical lightning mappers that share common design characteristics with GLM (e.g., OTD, TRMM/ISS LIS, FORTE, LMI, and MTG-LI). The exact details of how this manifests in their respective datasets will vary based on specific instrument and algorithm characteristics, but all of these sensors are/were likely vulnerable to undercounting flashes relative to an LMA during the intense (or anomalous) portions of thunderstorm lifecycles (e.g., Zhang and Cummins 2020). Thus, it is useful to explore the expected impacts of a future spaceborne sensor (or future

algorithm improvements to an existing sensor), which could be better designed to address this shortcoming.

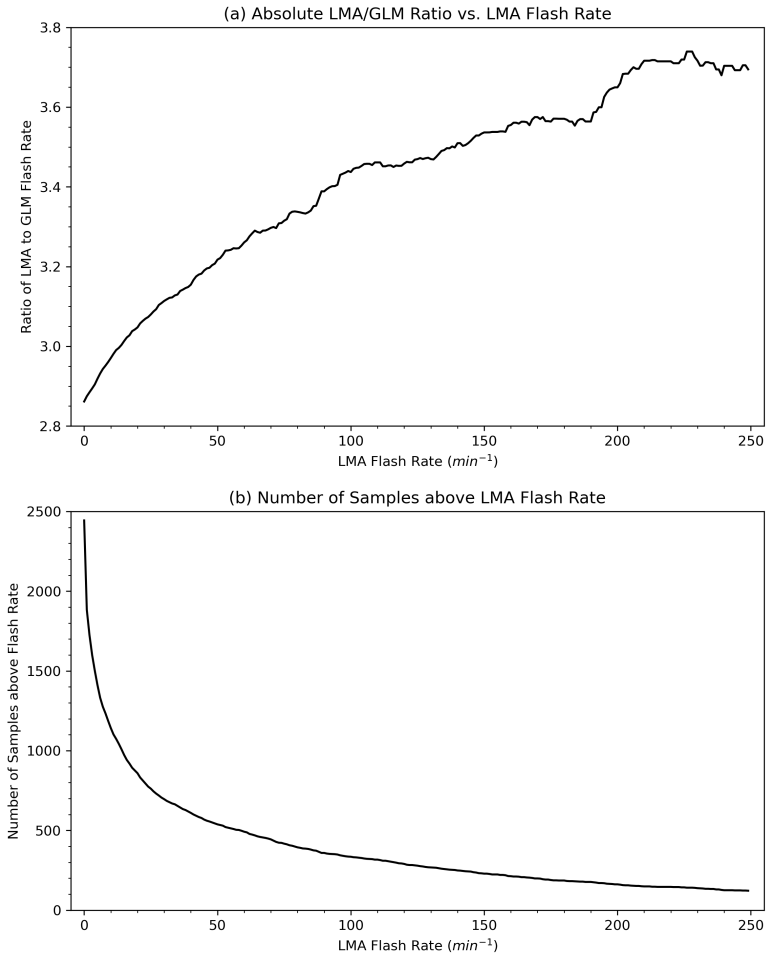

Figure 2. (a) Ratio of LMA to GLM flash rates, as a function of LMA flash rate. (b) Number of samples informing the time series in (a) as a function of LMA flash rate.

The improvements could be accomplished in a number of ways (e.g., more sensitive optics, additional complementary sensors/channels, improved spatiotemporal resolution, more optimized processing algorithms, etc.), but the present study is simply focused on aggregate improvements in flash detection capability, which can mean both increased DE as well as improved ability to distinguish between separate small flashes. For this analysis the focus will be on 0-100% improvements (in 10% bins) in flash identification relative to the LMA baseline. That

is, in a given minute, LMA flash rate will be x, GLM flash rate will be y, where $y < x$ and an "improved GLM" flash rate will be indicated as

$$y' = y + a\,(x - y),$$

where y' is the improved flash rate and a is the fractional improvement in flash detection capability (range 0.0-1.0, in 0.1 steps, as mentioned above).

Figure 3 shows an example of how this manifested during the 23 February 2019 case also studied in Fig. 1. The LMA time series (Fig. 3a) shows multiple intensifying and decay stages, and the LJ methodology identified a total of 6 jumps. The unimproved GLM time series (Fig. 3b) is significantly attenuated relative to the LMA, and flash rates and rate increases are too small to identify any LJs. However, a 30% improvement in flash detection capability (Fig. 3c) would bring the GLM closer in line with the LMA, and would reveal at least 3 LJs relatively close in time to the respective LMA-identified LJs. Though fundamental issues still persist even with these increased flash detections, there are demonstrable quantitative improvements in the ability for the spaceborne instrument to characterize thunderstorms.

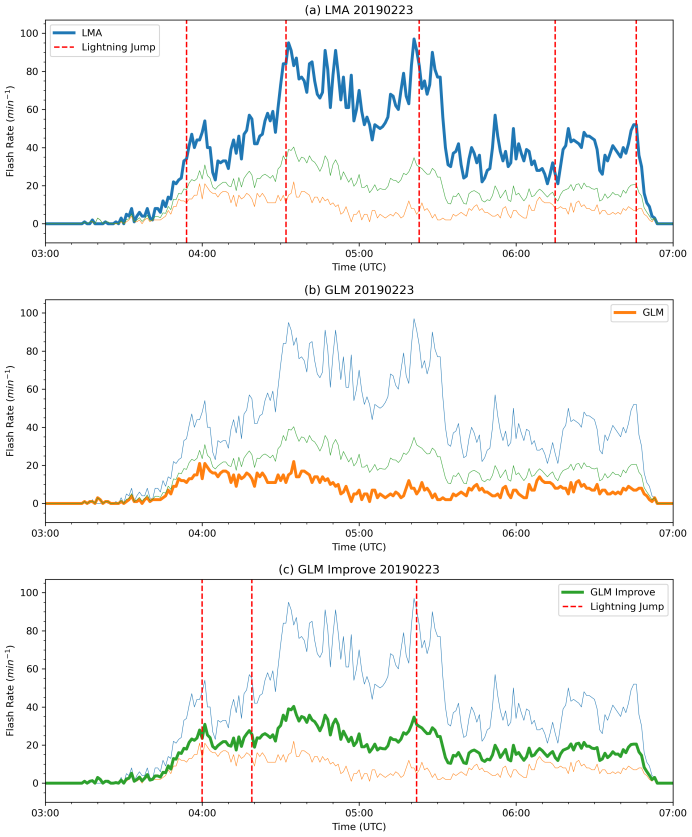

Figure 3. One-minute LMA, GLM, and improved GLM (assuming 30% increase in flash detectability relative to the LMA) for 23 February 2019. (a) Focused on LMA, with associated detected LJs. (b) focused on GLM, with no detected LJs. (c) Focused on improved GLM, with associated detected LJs.

Figure 4 shows the results for the entire December-April RELAMPAGO period, for 0-100% improvements in flash detection capability. The flash rate Spearman correlations (Fig. 4a)

increase rapidly, from ~0.84 to ~0.94, with only a modest 20% improvement in flash detection capability. Beyond 20%, the rate of improvement starts to decline as correlations asymptotically approach 1.0. Note that initial correlations with 0% improvement are below the values seen in Table 1, as the Fig. 4 analysis is based on 1-minute flash rates, not 10-minute rates. Unlike the asymptotic behavior in Fig. 4a, the ratio of "improved GLM" LJs to LMA-identified LJs responds approximately linearly to increased flash detection capability (Fig. 4b), though there is evidence of transient diminishing returns between 10 and 20%, before returning to a steeper rate of improvement within 20-100%. But overall, modest improvements in detectability lead to only modest gains. For example, a 20% improvement in flash detectability only nets a ~10% improvement in LJ detection (from the baseline ~50%). Meanwhile, to correctly identify 80% of LMA LJs, an improved GLM (or GLM-like sensor) would have to detect a whopping 50% more flashes.

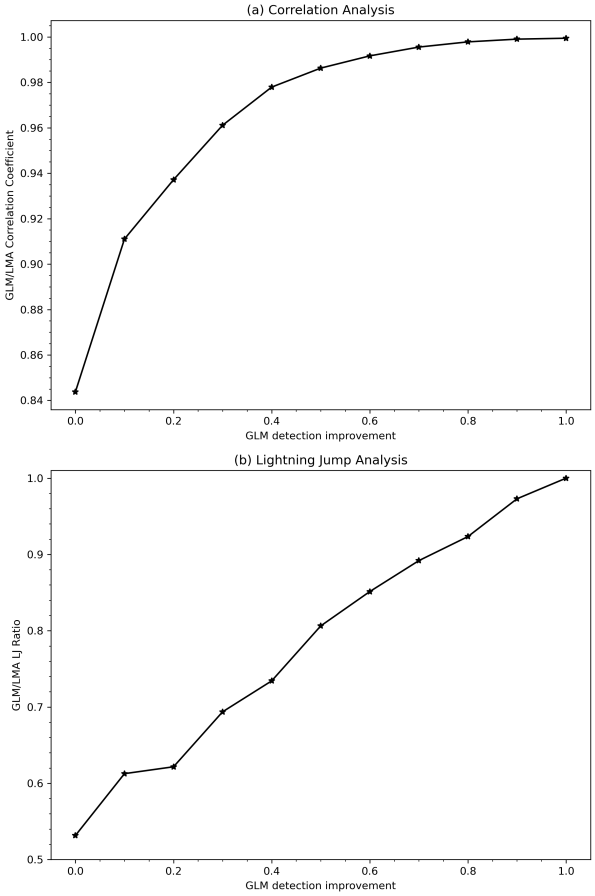

Figure 4. (a) Spearman correlations of 1-minute GLM vs. LMA flash rates, as a function of GLM detectability improvement, for December 2018 through April 2019. (b) Ratio of the total number of GLM- to LMA-detected LJs, as a function of GLM detectability improvement, for the same period.

4 Discussion and Conclusions

This study focused on validation of the GLM-16 sensor using data from an LMA deployed in north-central Argentina during 2018-2019, with special attention paid to DE as a

function of thunderstorm and lightning behavior. The analysis was confined to within 100 km of the LMA centroid, where performance of the ground-based network was maximized (Lang et al. 2020). While GLM DE was high overall (~75%), and GLM and LMA flash rates were highly correlated (r ~ 0.95), DE could vary significantly as thunderstorms evolved. In particular, GLM DE was negatively correlated (r ~ -0.5) with LMA flash rate; that is, as LMA flash rates increased within a thunderstorm, it became increasingly difficult for GLM to detect the additional lightning. GLM DE was significantly better (~10-20%) during the nighttime vs daytime, and for larger flashes vs. smaller (also ~10-20%). GLM DE was weakly correlated (r ~ 0.25) with the average number of points in LMA flashes, and this correlation was strongest in situations where GLM DE otherwise had negative influences (e.g., daytime). Periods of anomalous lightning (i.e., lightning associated with positively charged thunderstorm mid-levels, loosely defined) were associated with DE reductions of ~20-25%. GLM DE was weakly negatively correlated with flash altitude (r ~ -0.25), but this was very sensitive to spatiotemporal matching criteria and LMA points thresholds for flashes, which suggested the influence of multiple competing trends like anomalous lightning (worse expected DE), lower-altitude but larger stratiform lightning (better expected DE), and flash altitude increasing with thunderstorm intensification in normal-polarity storms (worse expected DE).

The overall high GLM DE occurred because this study allowed multiple LMA flashes to match to a single GLM flash. While this was a reasonable accommodation given the fundamentally different measurement technologies (one VHF- and ground-based, and capable of geolocation within 10s of meters, while the other spaceborne and optical with geolocation ~10 km), in reality LMA flashes outnumbered GLM flashes by about a factor of 3, and this ratio grew larger as LMA flash rate increased.

A sensitivity study was performed to examine the potential benefits of improved spaceborne detectability of these small flashes that are so ubiquitous in intense convection as measured by VHF sensors (e.g., Williams et al. 1999, Lang et al. 2000, Bruning and MacGorman 2013) as well as human-observed thunderstorms. In this context, detectability meant either improved flash DE or improved ability to distinguish between individual small flashes. Correlations improved significantly within the first 10-20% improvement in detectability, with more asymptotic behavior afterward. Meanwhile, the ability to identify LJs within the convection responded linearly to improved detectability. Overall, this suggests that sensor and/or algorithmic improvements that achieve modest improvements (~10-20%) in flash detectability could have a significant benefit for characterizing intense convection, but thereafter marginal improvements in detectability would have to be increasingly weighed against the costs associated with achieving that extra performance.

With spaceborne sensors that are always highly constrained by size, weight, and power requirements, a 10-20% increase in performance in the future as technology improves could be a reasonable goal. However, pushing beyond that likely would start to incur significant costs, which this study finds might only provide additional modest benefits, suggesting that the community involved in scientific analysis of intense/severe convection ought to consider other options as well. That is, simply focusing on improving flash rate measurements to better match those provided by LMAs will only provide diminishing returns relative to the expected costs associated with achieving that goal from spaceborne platforms. Improving the spaceborne technology is important, but improved algorithmic developments to better identify and characterize intense/severe convection using lightning observations are also needed (i.e., simply focusing on flash rates and identifying LJs is insufficient, from the spaceborne perspective).

503 Thankfully, there are a number of viable pathways to consider. Studies have found that
504 minimum and mean flash areas, as measured by spaceborne sensors like GLM, could provide
505 useful information about intensifying thunderstorms (e.g., Bruning et al. 2019). In addition,
506 group rate could provide information, since groups are a processing step removed from flashes in
507 GLM and related algorithms (Mach et al. 2007, Mach 2020), so analysis at that lower data level
508 reduces complexity. However, lightning group analysis needs to consider the presence (or lack
509 thereof) of stratiform lightning, which typically is associated with low flash rates but increased
510 group rates per flash (Peterson 2019). But more specifically, this study (in the context of many
511 others with similar results; e.g., Marchand et al. 2019) is a challenge to the lightning community
512 to develop algorithms that rely on more than just flash rates to characterize significant milestones
513 or processes in thunderstorm evolution, particularly when working with spaceborne lightning
514 observations.
515 This study has also demonstrated an innate 20-25% DE reduction with GLM when
516 anomalous lightning is occurring. This is consistent with related studies (e.g., Marchand et al.
517 2019, Murphy & Said 2020, Rutledge et a. 2020), and is on top of any additional DE reductions
518 associated with high flash rates. That is, an intense/severe anomalous storm with very high flash
519 rates could easily result in 20-30% DE for a spaceborne sensor like GLM (e.g., Fig. 1). This
520 result strongly argues for a spaceborne capability to measure lightning flash altitude, particularly
521 to identify the presence of anomalous storms. Indeed, the overall global frequency of anomalous
522 storms is poorly understood, even though it is highly likely that certain regions (e.g., Colorado
523 and similar climatological regimes) are disproportionately prone to their occurrence (e.g., Fuchs
524 et al. 2015). Lightning altitude may also play a role in terrestrial gamma-ray flash (TGF)
525 production (or at least detection of TGFs from space; e.g., Lopez et al. 2019) as well as the
526 production of transient luminous events (TLEs) such as sprites (e.g., Hu et al. 2002). One
527 potential option for this has been studies like Peterson et al. (2021), who used combined optical
528 and VHF measurements to measure lightning flash altitude from space.
529 The ability to resolve the vertical distribution of lightning from space (including
530 retrievals of lightning channel length; Koshak et al. 2014) also would greatly benefit studies of
531 lightning-produced nitrogen oxides (LNOx). LNOx, along with lightning-produced hydroxyl
532 radicals (OH), has important implications for the Earth's climate due to the species' strong
533 influence on the global lifecycles of tropospheric ozone and methane, which are powerful
534 greenhouse gases (Murray 2016, Wu et al. 2023).
535

Acknowledgments

The assistance of Dr. Bruno Lisboa Medina in clarifying anomalous time periods during RELAMPAGO is appreciated. The RELAMPAGO LMA deployment during 2018-2019 was successful due to the efforts of literally dozens of people and institutions from Argentina, the United States, and elsewhere. See Lang et al. (2020) for a full list of these individuals and organizations. Major funding for the RELAMPAGO LMA, as well as this study, came from the NOAA GOES-R Program, with additional support from the NASA Lightning Imaging Sensor (LIS) project. Partial support for this study also came from the NASA Instrument Incubator Program. The author declares no conflicts of interest. The views, opinions, and findings in this report are those of the author, and should not be construed as an official NASA or U.S. Government position, policy, or decision.

Open Research

RELAMPAGO LMA data may be obtained from http://dx.doi.org/10.5067/RELAMPAGO/LMA/DATA101. GLM Level-2 LCFA data may be obtained from https://doi.org/10.7289/V5KH0KK6. Analysis software used in this study was based on Python, and made used of major packages including numpy, scipy, matplotlib, pandas, xarray, h5py, and Jupyter, as well as more customized libraries like lmatools (https://github.com/deeplycloudy/lmatools). The specific analysis notebooks are undergoing the NASA open source release process and will be made available by formal publication in accordance with NASA Science Mission Directorate Policy Document 41a (https://science.nasa.gov/science-red/s3fs-public/atoms/files/SMD-information-policy-SPD-41a.pdf).

References

Bateman, M., & Mach, D. (2020). Preliminary detection efficiency and false alarm rate assessment of the Geostationary Lightning Mapper on the GOES-16 satellite. Journal of Applied Remote Sensing, 14(3), 032406-032406.

Bateman, M., Mach, D., & Stock, M. (2021). Further investigation into detection efficiency and false alarm rate for the geostationary lightning mappers aboard GOES-16 and GOES-17. Earth and Space Science, 8, e2020EA001237. https://doi.org/10.1029/2020EA001237

Blakeslee, R.J., Lang, T.J., Koshak, W.J., Buechler, D., Gatlin, P., Mach, D.M., Stano, G.T., Virts, K.S., Walker, T.D., Cecil, D.J., Ellett, W., Goodman, S.J., Harrison, S., Hawkins, D.L., Heumesser, M., Lin, H., Maskey, M., Schultz, C.J., Stewart, M., Bateman, M., Chanrion, O. and Christian, H. (2020), Three Years of the Lightning Imaging Sensor Onboard the International Space Station: Expanded Global Coverage and Enhanced Applications. J. Geophys. Res. Atmos., 125: e2020JD032918. https://doi.org/10.1029/2020JD032918

Bruning, E. C., and D. R. MacGorman, 2013: Theory and Observations of Controls on Lightning Flash Size Spectra. J. Atmos. Sci., 70, 4012–4029, https://doi.org/10.1175/JAS-D-12-0289.1.

582 Bruning, E., Tillier, C. E., Edgington, S. F., Rudlosky, S. D., Zajic, J., Gravelle, C., et al. (2019).
583 Meteorological imagery for the geostationary lightning mapper. Journal of Geophysical
584 Research: Atmospheres, 2019; 124: 14285– 14309. https://doi.org/10.1029/2019JD030874
585
586 Bruning, E. C., Weiss, S. A., & Calhoun, K. M. (2014). Continuous variability in thunderstorm
587 primary electrification and an evaluation of inverted-polarity terminology. Atmospheric
588 Research, 135, 274-284.
589
590 Cao, D.; Lu, F.; Zhang, X.; Yang, J. Lightning Activity Observed by the FengYun-4A Lightning
591 Mapping Imager. Remote Sens. 2021, 13, 3013. https://doi.org/10.3390/rs13153013
592
593 Chanrion, O., Neubert, T., Lundgaard Rasmussen, I. et al. The Modular Multispectral Imaging
594 Array (MMIA) of the ASIM Payload on the International Space Station. Space Sci Rev 215, 28
595 (2019). https://doi.org/10.1007/s11214-019-0593-y
596
597 Christian, H. J., et al., Global frequency and distribution of lightning as observed from space by
598 the Optical Transient Detector, J. Geophys. Res., 108(D1), 4005, doi:10.1029/2002JD002347,
599 2003.
600
601 Chronis, T., L. D. Carey, C. J. Schultz, E. V. Schultz, K. M. Calhoun, and S. J. Goodman, 2015:
602 Exploring Lightning Jump Characteristics. Wea. Forecasting, 30, 23–37,
603 https://doi.org/10.1175/WAF-D-14-00064.1.
604
605 Fuchs, B. R., Rutledge, S. A., Bruning, E. C., Pierce, J. R., Kodros, J. K., Lang, T. J.,
606 MacGorman, D. R., Krehbiel, P. R., and Rison, W. (2015), Environmental controls on storm
607 intensity and charge structure in multiple regions of the continental United States. J. Geophys.
608 Res. Atmos., 120, 6575– 6596. doi: 10.1002/2015JD023271.
609
610 GOES-R Algorithm Working Group and GOES-R Series Program (2018): NOAA GOES-R
611 Series Geostationary Lightning Mapper (GLM) Level 2 Lightning Detection: Events, Groups,
612 and Flashes. NOAA National Centers for Environmental Information. doi:10.7289/V5KH0KK6.
613
614 Gatlin, P. N., and Goodman S. J. , 2010: A total lightning trending algorithm to identify severe
615 thunderstorms. J. Atmos. Oceanic Technol., 27, 3–22, doi:10.1175/2009JTECHA1286.1.
616
617 Goodman, S. J., Blakeslee, R. J., Koshak, W. J., Mach, D., Bailey, J., Buechler, D., ... & Stano,
618 G. (2013). The GOES-R geostationary lightning mapper (GLM). Atmospheric research, 125, 34-
619 49.
620
621 Holmlund, K., and Coauthors, 2021: Meteosat Third Generation (MTG): Continuation and
622 Innovation of Observations from Geostationary Orbit. Bull. Amer. Meteor. Soc., 102, E990–
623 E1015, https://doi.org/10.1175/BAMS-D-19-0304.1.
624
625 Hu, W, Cummer, S., Lyons, W. A., and Nelson, T., Lightning charge moment changes for the
626 initiation of sprites, Geophys. Res. Lett., 29(8), doi:10.1029/2001GL014593, 2002.
627

628 Jacobson, A. R., & Light, T. E. L. (2012, February). Revisiting" Narrow Bipolar Event"
629 intracloud lightning using the FORTE satellite. In Annales geophysicae (Vol. 30, No. 2, pp. 389-
630 404). Göttingen, Germany: Copernicus Publications.
631
632 Koshak, W., Peterson, H., Biazar, A., Khan, M., & Wang, L. (2014). The NASA lightning
633 nitrogen oxides model (LNOM): Application to air quality modeling. Atmospheric Research,
634 135, 363-369.
635
636 Kummerow, C., W. Barnes, T. Kozu, J. Shiue, and J. Simpson, 1998: The Tropical Rainfall
637 Measuring Mission (TRMM) Sensor Package. J. Atmos. Oceanic Technol., 15, 809–817,
638 https://doi.org/10.1175/1520-0426(1998)015<0809:TTRMMT>2.0.CO;2.
639
640 Lang, Timothy, 2020. Remote sensing of Electrification, Lightning, And Mesoscale/microscale
641 Processes with Adaptive Ground Observations (RELAMPAGO) Lightning Mapping Array
642 (LMA). Dataset available online from the NASA Global Hydrometeorology Resource Center
643 DAAC, Huntsville, Alabama, U.S.A. DOI:
644 http://dx.doi.org/10.5067/RELAMPAGO/LMA/DATA101
645
646 Lang, T. J., & Bang, S. D. (2022). Exploring the scientific utility of combined spaceborne Lidar
647 and Lightning observations of thunderstorms. Earth and Space Science, 9, e2022EA002400.
648 https://doi.org/10.1029/2022EA002400
649
650 Lang, T. J., and Coauthors, 2020: The RELAMPAGO Lightning Mapping Array: Overview and
651 Initial Comparison with the Geostationary Lightning Mapper. J. Atmos. Oceanic Technol., 37,
652 1457–1475, https://doi.org/10.1175/JTECH-D-20-0005.1.
653
654 Lang, T. J., S. A. Rutledge, J. E. Dye, M. Venticinque, P. Laroche, and E. Defer, 2000:
655 Anomalously Low Negative Cloud-to-Ground Lightning Flash Rates in Intense Convective
656 Storms Observed during STERAO-A. Mon. Wea. Rev., 128, 160–173,
657 https://doi.org/10.1175/1520-0493(2000)128<0160:ALNCTG>2.0.CO;2.
658
659 López, J. A., Montanyà, J., van der Velde, O. A., Pineda, N., Salvador, A., Romero, D., et al.
660 (2019). Charge structure of two tropical thunderstorms in Colombia. Journal of Geophysical
661 Research: Atmospheres, 124, 5503– 5515. https://doi.org/10.1029/2018JD029188
662
663 Mach, D. M. (2020). Geostationary Lightning Mapper clustering algorithm stability. Journal of
664 Geophysical Research: Atmospheres, 125, e2019JD031900.
665 https://doi.org/10.1029/2019JD031900
666
667 Mach, D. M., Christian, H. J., Blakeslee, R. J., Boccippio, D. J., Goodman, S. J., and Boeck, W.
668 L. (2007), Performance assessment of the Optical Transient Detector and Lightning Imaging
669 Sensor, J. Geophys. Res., 112, D09210, doi:10.1029/2006JD007787.
670
671 Marchand, M., Hilburn, K., & Miller, S. D. (2019). Geostationary lightning mapper and Earth
672 networks lightning detection over the contiguous United States and dependence on flash

673 characteristics. Journal of Geophysical Research: Atmospheres, 124, 11552– 11567.
674 https://doi.org/10.1029/2019JD031039
675
676 Medina, B. L., Carey, L. D., Bitzer, P. M., Lang, T. J., & Deierling, W. (2022). The Relation of
677 environmental conditions with charge structure in central Argentina thunderstorms. Earth and
678 Space Science, 9, e2021EA002193. https://doi.org/10.1029/2021EA002193
679
680 Medina, B. L., Carey, L. D., Lang, T. J., Bitzer, P. M., Deierling, W., & Zhu, Y. (2021).
681 Characterizing charge structure in Central Argentina thunderstorms during RELAMPAGO
682 utilizing a new charge layer polarity identification method. Earth and Space Science, 8,
683 e2021EA001803. https://doi.org/10.1029/2021EA001803
684
685 Murphy, M. J., & Said, R. K. (2020). Comparisons of lightning rates and properties from the
686 U.S. National Lightning Detection Network (NLDN) and GLD360 with GOES-16 Geostationary
687 Lightning Mapper and Advanced Baseline Imager data. Journal of Geophysical Research:
688 Atmospheres, 125, e2019JD031172. https://doi.org/10.1029/2019JD031172
689
690 Murray, L.T. Lightning NO x and Impacts on Air Quality. Curr Pollution Rep 2, 115–133
691 (2016). https://doi.org/10.1007/s40726-016-0031-7
692
693 Nesbitt, S. W., and Coauthors, 2021: A Storm Safari in Subtropical South America: Proyecto
694 RELAMPAGO. Bull. Amer. Meteor. Soc., 102, E1621–E1644, https://doi.org/10.1175/BAMS-
695 D-20-0029.1.
696
697 Neubert, T., Østgaard, N., Reglero, V. et al. The ASIM Mission on the International Space
698 Station. Space Sci Rev 215, 26 (2019). https://doi.org/10.1007/s11214-019-0592-z
699
700 Peterson, M. (2019). Research applications for the Geostationary Lightning Mapper operational
701 lightning flash data product. Journal of Geophysical Research: Atmospheres, 124, 10205–
702 10231. https://doi.org/10.1029/2019JD031054
703
704 Peterson, M. (2020). Removing solar artifacts from Geostationary Lightning Mapper data to
705 document lightning extremes. Journal of applied remote sensing, 14(3), 032402-032402.
706
707 Peterson, M. (2021a). Holes in optical lightning flashes: Identifying poorly transmissive clouds
708 in lightning imager data. Earth and Space Science, 8, e2020EA001294.
709 https://doi.org/10.1029/2020EA001294
710
711 Peterson, M., 2021b: Where Are the Most Extraordinary Lightning Megaflashes in the
712 Americas?. Bull. Amer. Meteor. Soc., 102, E660–E671, https://doi.org/10.1175/BAMS-D-20-
713 0178.1.
714
715 Peterson, M., Light, T. E. L., & Shao, X.-M. (2021). Combined optical and radio-frequency
716 perspectives on a hybrid Cloud-to-Ground lightning flash observed by the FORTE satellite.
717 Journal of Geophysical Research: Atmospheres, 126, e2020JD034152.
718 https://doi.org/10.1029/2020JD034152

719
720 Quick, M. G., Christian, H. J., Virts, K. S., & Blakeslee, R. J. (2020). Airborne radiometric
721 validation of the geostationary lightning mapper using the Fly's Eye GLM Simulator. Journal of
722 Applied Remote Sensing, 14(4), 044518-044518.
723
724 Rison, W., Thomas, R. J., Krehbiel, P. R., Hamlin, T., and Harlin, J.: A GPS-based three-
725 dimensional lightning mapping system: Initial observations in central New Mexico, Geophys.
726 Res. Lett., 26, 3573–3576, https://doi.org/10.1029/1999GL010856, 1999.
727
728 Rudlosky, S. D., Goodman, S. J., Virts, K. S., & Bruning, E. C. (2019). Initial geostationary
729 lightning mapper observations. Geophysical Research Letters, 46, 1097– 1104.
730 https://doi.org/10.1029/2018GL081052
731
732 Rudlosky, S. D., and K. S. Virts, 2021: Dual Geostationary Lightning Mapper Observations.
733 Mon. Wea. Rev., 149, 979–998, https://doi.org/10.1175/MWR-D-20-0242.1.
734
735 Rust, W. D., MacGorman, D. R., Bruning, E. C., Weiss, S. A., Krehbiel, P. R., Thomas, R. J., ...
736 & Harlin, J. (2005). Inverted-polarity electrical structures in thunderstorms in the Severe
737 Thunderstorm Electrification and Precipitation Study (STEPS). Atmospheric Research, 76(1-4),
738 247-271.
739
740 Rutledge, S. A., Hilburn, K. A., Clayton, A., Fuchs, B., & Miller, S. D. (2020). Evaluating
741 Geostationary Lightning Mapper flash rates within intense convective storms. Journal of
742 Geophysical Research: Atmospheres, 125, e2020JD032827.
743 https://doi.org/10.1029/2020JD032827
744
745 Schultz, C. J., L. D. Carey, E. V. Schultz, and R. J. Blakeslee, 2015: Insight into the Kinematic
746 and Microphysical Processes that Control Lightning Jumps. Wea. Forecasting, 30, 1591–1621,
747 https://doi.org/10.1175/WAF-D-14-00147.1.
748
749 Schultz, C. J., L. D. Carey, E. V. Schultz, and R. J. Blakeslee, 2017: Kinematic and
750 Microphysical Significance of Lightning Jumps versus Nonjump Increases in Total Flash Rate.
751 Wea. Forecasting, 32, 275–288, https://doi.org/10.1175/WAF-D-15-0175.1.
752
753 Schultz, C. J., W. A. Petersen, and L. D. Carey, 2009: Preliminary Development and Evaluation
754 of Lightning Jump Algorithms for the Real-Time Detection of Severe Weather. J. Appl. Meteor.
755 Climatol., 48, 2543–2563, https://doi.org/10.1175/2009JAMC2237.1.
756
757 Soler, S., Gordillo-Vázquez, F. J., Pérez-Invernón, F. J., Luque, A., Li, D., Neubert, T., et al.
758 (2021). Global frequency and geographical distribution of nighttime streamer corona discharges
759 (BLUEs) in thunderclouds. Geophysical Research Letters, 48, e2021GL094657.
760 https://doi.org/10.1029/2021GL094657
761
762 Suszcynsky, D. M., Kirkland, M. W., Jacobson, A. R., Franz, R. C., Knox, S. O., Guillen, J. L.
763 L., and Green, J. L. (2000), FORTE observations of simultaneous VHF and optical emissions

764 from lightning: Basic phenomenology, J. Geophys. Res., 105(D2), 2191– 2201,
765 doi:10.1029/1999JD900993.
766
767 Thomas, R. J., Krehbiel, P. R., Rison, W., Hunyady, S. J., Winn, W. P., Hamlin, T., and Harlin,
768 J. (2004), Accuracy of the Lightning Mapping Array, J. Geophys. Res., 109, D14207,
769 doi:10.1029/2004JD004549.
770
771 Virts, K. S., and W. J. Koshak, 2020: Mitigation of Geostationary Lightning Mapper Geolocation
772 Errors. J. Atmos. Oceanic Technol., 37, 1725–1736, https://doi.org/10.1175/JTECH-D-19-
773 0100.1.
774
775 Virts, K. S., and W. J. Koshak, 2023: Monte Carlo Simulations for Evaluating the Accuracy of
776 Geostationary Lightning Mapper Detection Efficiency and False Alarm Rate Retrievals. J.
777 Atmos. Oceanic Technol., 40, 219–235, https://doi.org/10.1175/JTECH-D-22-0050.1.
778
779 Wiens, K. C., S. A. Rutledge, and S. A. Tessendorf, 2005: The 29 June 2000 Supercell Observed
780 during STEPS. Part II: Lightning and Charge Structure. J. Atmos. Sci., 62, 4151–4177,
781 https://doi.org/10.1175/JAS3615.1.
782
783 Williams, E. R., and Coauthors, 1999: The behavior of total lightning activity in severe Florida
784 thunderstorms. Atmos. Res., 51, 245–265, doi:10.1016/S0169-8095(99)00011-3.
785
786 Wu, Y., Pour-Biazar, A., Koshak, W. J., & Cheng, P. (2023). LNOx emission model for air
787 quality and climate studies using satellite lightning mapper observations. Journal of Geophysical
788 Research: Atmospheres, 128, e2022JD037406. https://doi.org/10.1029/2022JD037406
789
790 Zhang, D., & Cummins, K. L. (2020). Time evolution of satellite-based optical properties in
791 lightning flashes, and its impact on GLM flash detection. Journal of Geophysical Research:
792 Atmospheres, 125, e2019JD032024. https://doi.org/10.1029/2019JD032024
793

Figure 1.

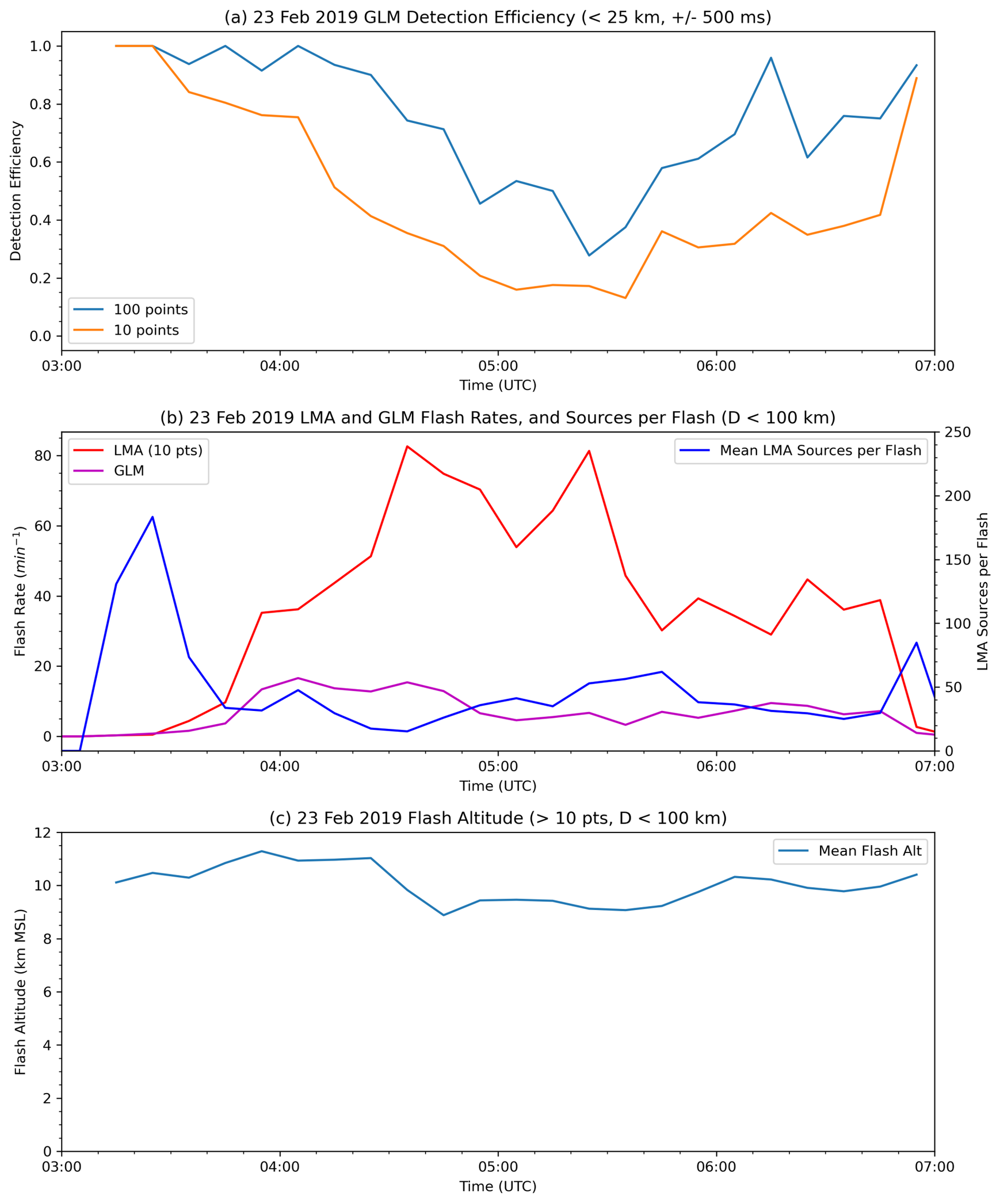
(a) 23 Feb 2019 GLM Detection Efficiency (< 25 km, +/- 500 ms)
Detection Efficiency
1.0
0.8
0.6
0.4
0.2
0.0
100 points
10 points
03:00
04:00
05:00
06:00
07:00
Time (UTC)
(b) 23 Feb 2019 LMA and GLM Flash Rates, and Sources per Flash (D < 100 km)
LMA (10 pts)
GLM
Mean LMA Sources per Flash
Flash Rate (min⁻¹)
80
60
40
20
0
250
200
150
100
50
0
LMA Sources per Flash
03:00
04:00
05:00
06:00
07:00
Time (UTC)
(c) 23 Feb 2019 Flash Altitude (> 10 pts, D < 100 km)
Mean Flash Alt
Flash Altitude (km MSL)
12
10
8
6
4
2
0
03:00
04:00
05:00
06:00
07:00
Time (UTC)

Figure 2.

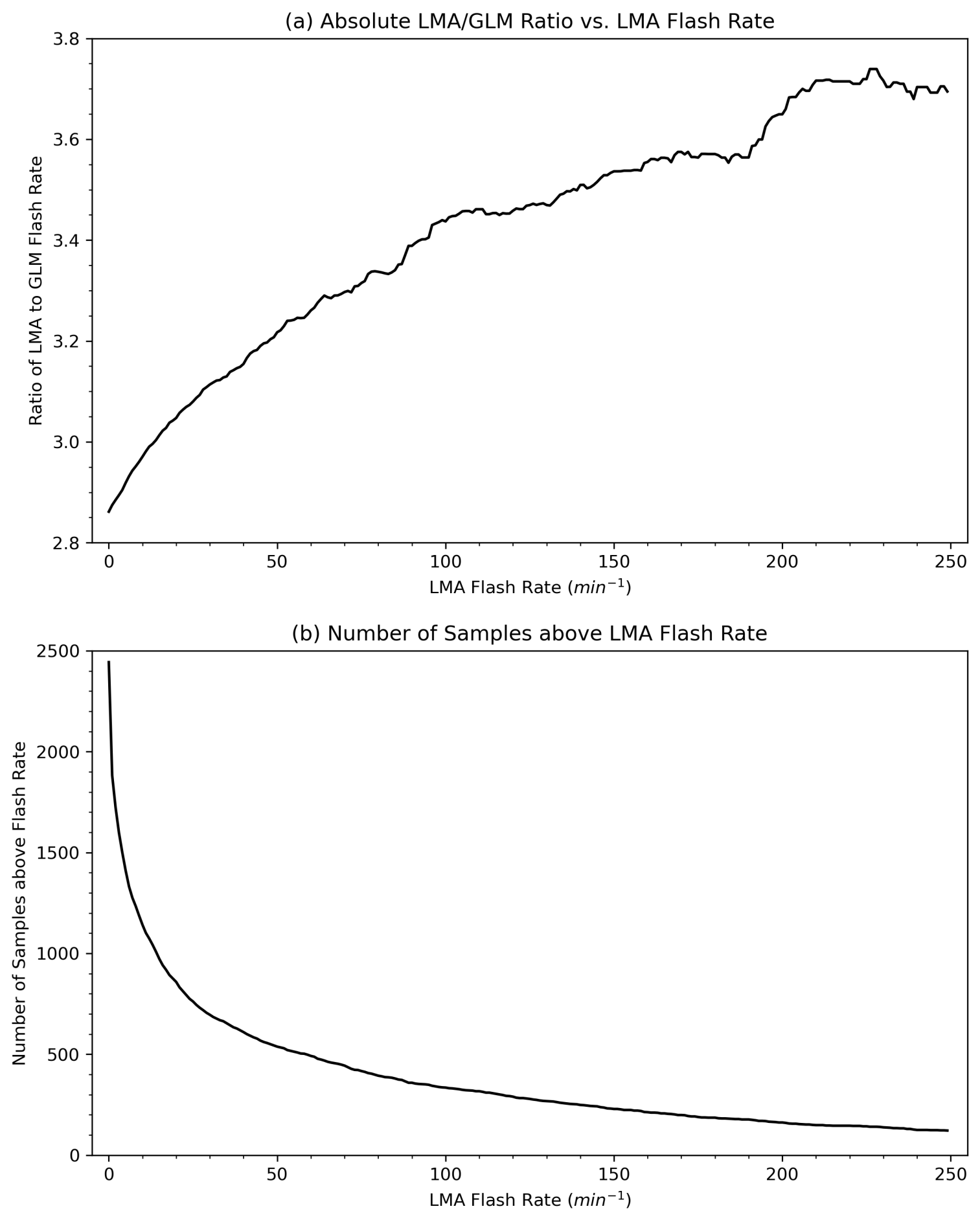
(a) Absolute LMA/GLM Ratio vs. LMA Flash Rate
Ratio of LMA to GLM Flash Rate
LMA Flash Rate (min^{-1})
(b) Number of Samples above LMA Flash Rate
Number of Samples above Flash Rate
LMA Flash Rate (min^{-1})

Figure 3.

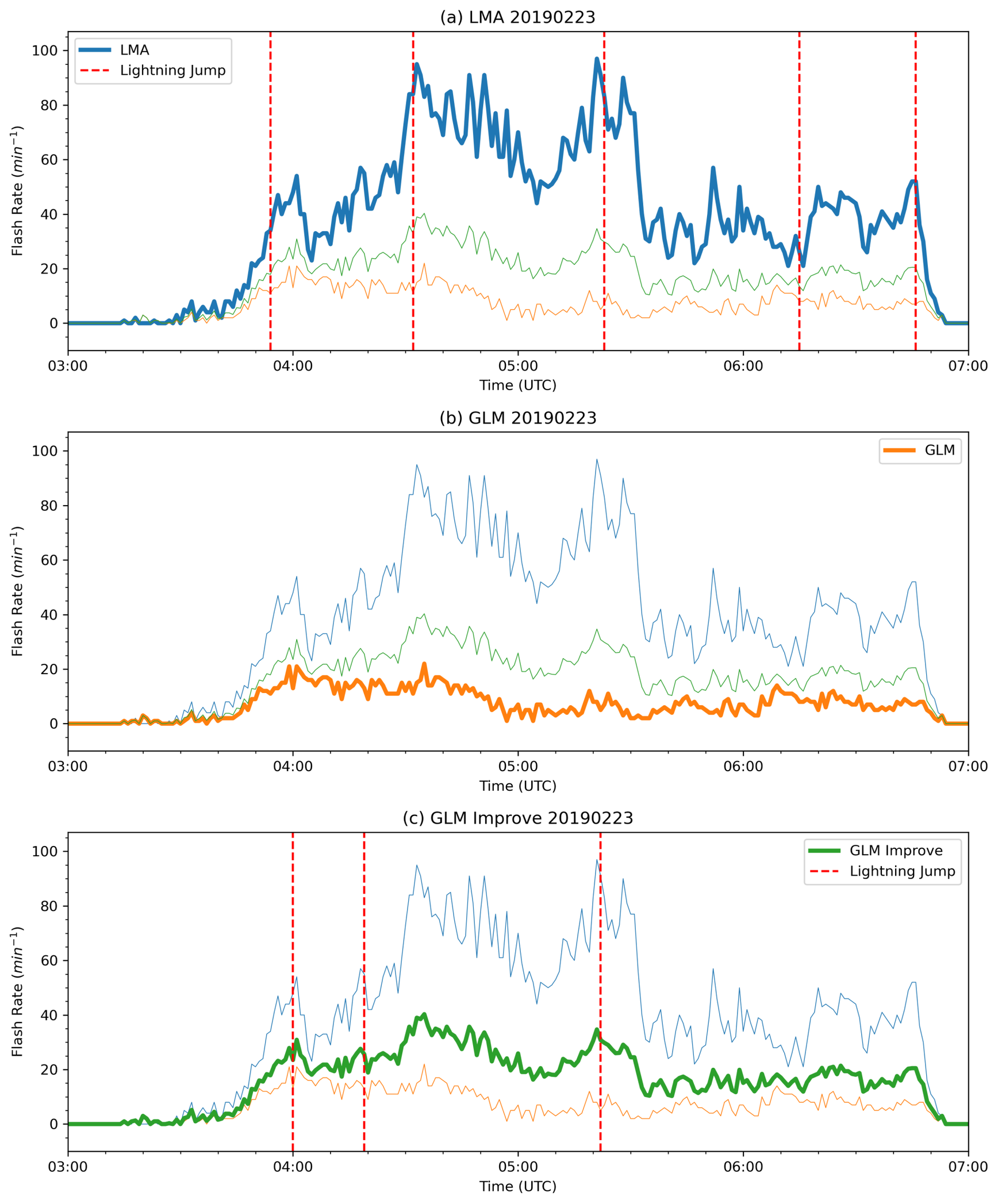
(a) LMA 20190223
LMA
Lightning Jump
Flash Rate (min^{-1})
Time (UTC)
03:00
04:00
05:00
06:00
07:00
(b) GLM 20190223
GLM
Flash Rate (min^{-1})
Time (UTC)
(c) GLM Improve 20190223
GLM Improve
Lightning Jump
Flash Rate (min^{-1})
Time (UTC)

Figure 4.

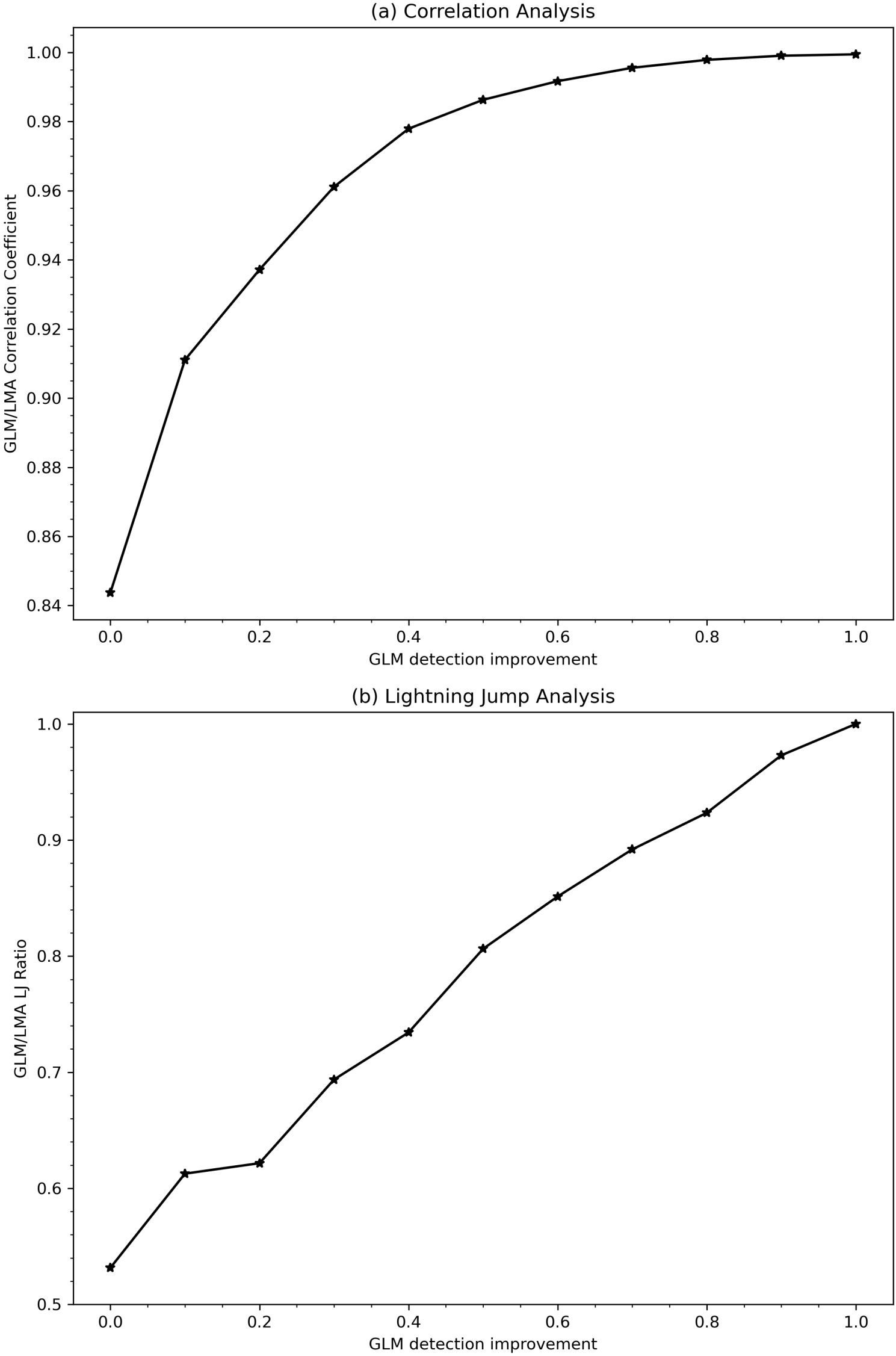
(a) Correlation Analysis
GLM/LMA Correlation Coefficient
1.00
0.98
0.96
0.94
0.92
0.90
0.88
0.86
0.84
0.0
0.2
0.4
0.6
0.8
1.0
GLM detection improvement
(b) Lightning Jump Analysis
GLM/LMA LJ Ratio
1.0
0.9
0.8
0.7
0.6
0.5
0.0
0.2
0.4
0.6
0.8
1.0
GLM detection improvement